Effect of the Richardson Number on Flow and Heat Transfer in a Cylinder Filled with Cu-Water Nano-fluid at Different Nanoparticle Concentrations

*SANGOTAYO, EO; OGIDIGA, JO

Department of Mechanical Engineering, Ladoke Akintola University of Technology, Ogbomoso, Nigeria

Corresponding Author Email: eosangotayo@lautech.edu.ng
Other Author Email: joel.ogidiga@yahoo.com

ABSTRACT: Fluid circulation and thermal exchange properties via integrated natural and artificial convection within a container have attracted considerable interest due to its many industrial uses. This present work concentrates on determining the effect of the Richardson number on flow and heat transfer in a cylinder filled with Cu-Water nanofluid at different nanoparticle concentrations. The governing equations: continuity and Navier Stoke fields were discretized using the finite difference approach and simulated in C++ programming language. In this work, the Richardson parameter ranged from $2.6*10^4$ to $2.8*10^4$, while the concentration of Cu nanoparticles ranged from 1% to 10%, and the results are presented as Nusselt number, vorticity, and stream function profiles. The results reveal that the maximum Richardson value is 2.76×10^4 at the nanoparticle volume of 0.04, resulting in a considerable increase in the convective heat transfer rate. Furthermore, as the Richardson parameters increase, the Nusselt number in the nanofluid increases exponentially while the local drag coefficient decreases. The stream function, longitudinal velocity and circulation increase as the Richardson parameters grow. The technical design for air turbulence prediction involves an understanding of the Richardson-driven connection as a mix of wind speed and convective stability variables.

Understanding the heat characteristics of a system enables designers to construct systems with high dependability and minimal energy consumption. Heat transfer in thermal technologies is a crucial topic in the industry. Although many industrial circumstances have intricate geometry, basic geometries such as cylinders can be found in a range of applications, such as chilling electronic equipment, air conditioning, and solar devices, Khodadadi and Hosseinizadeh, (2007); Mastiani *et al*., (2015). Consequently, numerous researchers have been attracted to the study of closed enclosures to examine the fluid motion and thermal behavior of a system for diverse fluids, shapes, and operating conditions, such as partly hot. In a number of these cases, the source of the flow is a mix of forced convection and free convection, which was addressed using computational approaches because computer modeling is far less expensive than experimentation, (Umavathi and Beg, 2021); Lin *et al*., 2008). It is often important to swiftly remove heat from and cool equipment in a variety of applications. Price, safety, and environmental restrictions limit the variety of fluids available for this application. It is affordable and readily accessible, yet its properties are insufficient for removing heat from certain equipment. Due to this, water is selected as the coolant. To resolve this issue, it is required to enhance the thermal properties of water using technologies that are both safe and cost-effective. Although most liquids possess comparable qualities, such as a large heat capacity and a small conductivity coefficient, Taylor *et al*. (2011) introduced additional liquid to water to enhance its

properties. Incorporating nanoparticles with a particulate size of less than 100 nm into fluids to achieve the preferred features is a typical method for increasing the thermal properties of fluids, (Selimefendigil and Oztop, 2018). Nano-particles usually consist of particles of solid metals, such as Ag, Cu, and Au, or metal oxides, such as Al_2O_3, Fe_2O_3, and SiO_2, which can improve heat capacity and thermal conductivity, (Sheikholeslami and Rokni, 2017). Choi *et al.* (1995) presented the usage of nanoparticles in heat transmission and revealed that the introduction of nanofluid boost thermal conductivity by 7%. Sherement and Pop (2015) conducted a study utilizing Buongiorno's theoretical model to determine the most significant parameter coupled convection heat exchange in a lid-driven nanofluid reservoir. It was found that the Richardson factor plays the most important influence on flow and heat transfer qualities. Tiwari and Das (2007) explored mixed convective and its influence on the Nusselt number using a chamber containing Cu water fluid. The outcome revealed that the mean Nusselt value increased substantially while the Richardson number remained steady. Mastiani *et al.* (2017) examined mixed convection in a cube-shaped box containing water and copper nanofluid. Researchers evaluated the impact of density on the Nusselt value for a variation of lid speeds and at large Richardson numbers and discovered that the impact of density inversion becomes increasingly substantial. Billah *et al.* (2013) analyzed the non-steady combined heat exchange in a triangular cavity at various angles. The solid volume percent was discovered to affect temperature and flow field. Nasrin and Parvin (2012) analyzed the impact of various nano solid concentrations and aspect ratios on the stream pattern and isotherm paths of water-Cu nanofluid under buoyancy-driven motion in a trapezoidal chamber. The results indicated that the heat and flow trends are quite sensitive to the aspect ratio of the design. Kareem and Gao (2017) examined the impact of different nanoparticles and water on the rate of combined convection heat transmission in a lid-driven trapezoidal enclosure. It was established that the Al_2O_3, TiO_2, SiO_2, and CuO water combination had the maximum Nusselt number and the Nusselt value enlarges as the nanoparticle volumetric fraction amplifies. Basak *et al.* (2009) examined the effect of Reynolds and Grashof values on laminar flow utilizing the finite element method for homogeneous and heterogeneous heating from the base of a square chamber with mixed convection. It was established that consistent heating is more efficient than inconsistent heating and that regular heating increases the Nusselt number. Alrashed *et al.* (2018) investigated entropy formation and combined convection in an unlock chamber using an isothermal

slab to heat the nanofluid. The study revealed that the Richardson number plays a crucial role in entropy generation. Hussain *et al.* (2017) investigated the impact of nanoparticle volumetric fraction on temperature gradient patterns. The result revealed that raising the volumetric fraction to eight percent increase the local Nusselt value by up to fifty percent. Sangotayo and Hunge (2019) studied the influence of nanoparticle volumetric fraction on thermophysical properties and convective heat transport in a square container filled with CuO nanofluid. It has been discovered that the size of nanomaterials has a considerable impact on heat transfer. Khanafer and Aithal (2017) studied the effect of a spinning tube on the combined convection in a lid-driven hole employing Al_2O_3, TiO_2, and Cu nanomaterials to fill the void; It was revealed that water and copper have the greatest rate of heat transport. The ideal design for manufacturing systems by utilizing an optimization method, such as a genetic approach or a synthetic algorithm was described in Meymian, *et al.* (2018). The implementation of nanofluids as phase shift materials has been the focus of contemporary research. Nguyen-Thoi *et al.*, (2019)**;** Waqas *et al.*, (2019); Yousif *et al.*, (2019)**.** All of these researches explored the characteristics of forced, natural, or combined convection in 2D or cubical tunnels with different boundary settings and nanomaterials. No previous work, to the author's knowledge, has explored laminar combined convection in a cylindrical tube containing nanofluid under isothermal border conditions. There has been less research on the influence of the Richardson parameter on the fluid flow and thermal features of nanofluids, even though various scientists have created models for calculating the granular size of nanofluids. Several industries, such as turbomachinery and electrical device cooling, utilize the tubular cavity. This observed gap in the literature motivated the writers of this paper. This present work concentrates on determining the influence of the Richardson number on flow pattern and heat transport in a cylinder filled with Cu-Water nanofluid at different nanoparticle concentrations.

MATERIALS AND METHODS

Physical configuration: The two-dimensional steady laminar boundary layer flow of an incompressible Newtonian fluid with viscous fluid on the surface of the cylinder is illustrated in Fig. 1. T_w is the constant surface temperature, while T_∞ is the free stream temperature (where $T_w > T_\infty$). The surface velocity is U_w in the same direction as the fluid with velocity U_∞ in the free stream zone, where $U_\infty > U_w$. The liquid consists of copper nanoparticles suspended in water. The thermophysical characteristics are listed in Table 1.
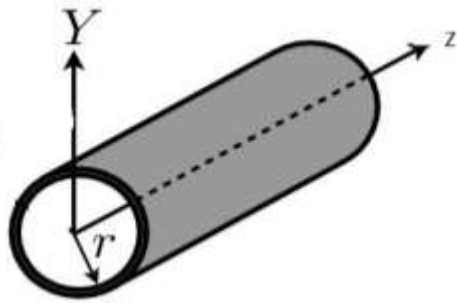
Fig. 1: A schematic representation illustrating the physical state and boundary conditions of an isothermal cylinder wall

Table1: Thermo-physical characteristics of Cu-water nanofluid

	Density (kgm^{-3})	Heat Capacity (J/kg^{-1}K^{-1})	Thermal Conductivity (Wm^{-1}K^{-1})	Thermal expansion (K^{-1})	Viscosity
H$_2$O	997.1	4179	0.613	21x10^{-5}	9.09x10^{-5}
Cu	8954	383	400	1.67x10^{-5}	

Mathematical Expression: In this problem, it is assumed that the fluid is incompressible, that the base fluid (water) and Cu nanoparticles are in thermal equilibrium, and that no slip requirement exists between them. Based on the assumption that the flow is laminar, there are no internal thermal sources, the flow is two-dimensional, and the Boussinesq approach applies, the governing formulas were solved. The flow is believed to be stable, viscous dissipation-free, and incompressible. The gravitational strength acts vertically downward, but the radiation effect is negligible. Flow-regulating formulas consist of mass and momentum conservation formulas at every location along the continuum, Patankar (1980).

A two-dimensional cylindrical domain is defined by this formula in Eq.[1]
Continuity equation:

$$\frac{\partial u}{\partial z} + \frac{\partial v}{\partial r} = 0 \qquad (1)$$

Eq. (2 and 3) are Navier-Stokes models in the r- and z-coordinates.

$$u\frac{\partial v}{\partial z} + v\frac{\partial v}{\partial r} = -\frac{1}{\rho_{nf}}\frac{\partial p}{\partial r} + \frac{\mu_{nf}}{\rho_{nf}}\left(\frac{\partial^2 v}{\partial z^2} + \frac{\partial^2 v}{\partial r^2}\right)$$
$$+ \frac{(\rho\beta)_{nf}}{\rho_{nf}} g(T - T_c) \qquad (2)$$

Where $\frac{(\rho\beta)_{nf}}{\rho_{nf}} g(T - T_c)$ is z-coordinate force per unit volume?

The formula for thermal energy exchange using Eq. (3)

$$\rho c_p \left(u\frac{\partial T}{\partial r} + v\frac{\partial T}{\partial z}\right) = k\left(\frac{\partial T}{\partial r^2} + \frac{\partial T}{\partial z^2}\right) \qquad (3)$$

Where the nanofluid heat capacity is $(C_p)_{nf}$, density is ρ_{nf}, thermal expansion coefficient is $(\beta)_{nf}$, and thermal diffusivity is (α_{nf}) as expressed in Eq. (5-10) (Kalbasi and Saeedi, 2012)

$$\rho_{nf} = (1 - \varphi)\rho_f + \varphi\rho_s \qquad (5)$$

$$(\rho C_p)_{nf} = (1 - \varphi)(\rho C_p)_f + \varphi(\rho C_p)_s \qquad (6)$$

$$(\rho\beta)_{nf} = (1 - \varphi)(\rho\beta)_f + \varphi(\rho\beta)_s (7)$$

$$\alpha_{nf} = \frac{k_{nf}}{(\rho C_p)_{nf}} \qquad (8)$$

The effective viscosity of the nanofluid is calculated using the Brinkman theory in Eq. (9) Kalbasi and Saeedi (2012)

$$\mu_{eff} = \frac{\mu_f}{(1 - \varphi)^{2.5}} \qquad (9)$$

The active thermal conductivity (k$_{nf}$) of the nanofluid-containing nanospheres is computed using Eq. (10). (Kalbasi and Saeedi. 2012)

$$\frac{k_{nf}}{k_f} = \frac{k_s + 2k_f - 2\varphi(k_f - k_s)}{k_f + 2K_s + \varphi(k_f - k_s)} \qquad (10)$$

Methods of Examination and Strategies of Resolution: The Navier-Stokes models are a type of partial derivative problem that, depending on the application, can be hyperbolic, elliptic, or parabolic. The vorticity-stream parameter method or the primitive-variable technique can be used to analyze these formulas. Formulas (2) and (3) are simplified to vorticity transport formulas using the vorticity-stream feature approach by removing the pressure gradient notions between the two, employing the continuity model (1), and expressing the vorticity's scalar worth in the two-dimensional polar coordinates scheme described by the vorticity-stream feature. Eq. (11)

$$\omega = \frac{\partial v}{\partial r} - \frac{\partial u}{\partial z}. \qquad (11)$$

The resultant statement, equation, is the dimensional vorticity transfer (12)

$$u\frac{\partial \omega}{\partial r} + v\frac{\partial \omega}{\partial z} = -\beta g\frac{\partial T}{\partial r} + \upsilon\left(\frac{\partial^2 \omega}{\partial r^2} + \frac{\partial^2 \omega}{\partial z^2}\right) \quad (12)$$

The differential of the stream function is used to describe the velocity field in two-dimensional cylindrical coordinate, ψ, Eq. (13)

$$u = \frac{\partial \psi}{\partial z}, \quad v = -\frac{\partial \psi}{\partial r} \quad (13)$$

When substituted in equation (11), it provides the Poisson formula (Eq.14)

$$\omega = -\left(\frac{\partial^2 \psi}{\partial r^2} + \frac{\partial^2 \psi}{\partial z^2}\right) \quad (14)$$

The resulting transfer formula, energy model, and needed operating situation were all converted to a non-dimensional formulation for a variety of physical situations utilizing U_W, $\psi_W L$, L, ω_W/L and $(T_w - T_\infty)$, respectively for velocity, stream function, length, vorticity, and temperature, [29].

$$R = \frac{r}{L}, \quad Z = \frac{z}{L}, \quad U = \frac{u}{U_w}, \quad V = \frac{v}{U_w},$$

$$\theta = \frac{(T - T_\infty)}{(T_w - T_\infty)}, \quad \Psi = \frac{\psi}{U_w L}, \quad \Omega = \frac{\omega}{U_w/L},$$

The following are the normalized formulas for the R- and Z-velocity elements, the stream component, vortex shedding, and energy transit as expressed in Eq. (15 - 18):

$$u = \frac{\partial \varphi}{\partial z}, \quad V = -\frac{\partial \varphi}{\partial R} \quad (15)$$

$$\omega = -\frac{\partial^2 \varphi}{\partial Z^2} - \frac{\partial^2 \varphi}{\partial R^2} \quad (16)$$

$$u\frac{\partial \omega}{\partial Z} - V\frac{\partial \omega}{\partial R} = Ra\,Pr\left(\frac{\beta_{nf}}{\beta_f}\right)\frac{\partial \theta}{\partial Z} + \left(\frac{\mu_{nf}}{\rho_{nf}\alpha_{nf}}\right)\left(\frac{\partial^2 \omega}{\partial Z^2} + \frac{\partial^2 \omega}{\partial R^2}\right) \quad (17)$$

Where $Pr = {V_f}/{\alpha_f}$, $Pr_{nf} = {V_{nf}}/{\alpha_{nf}}$

$$u\frac{\partial \theta}{\partial Z} + V\frac{\partial \theta}{\partial R} = C\left(\frac{\alpha_{nf}}{\alpha_f}\right)\left(\frac{\partial^2 \theta}{\partial Z^2} + \frac{\partial^2 \theta}{\partial R^2}\right) \quad (18)$$

Where μ represents dynamic viscosity, k represents thermal conductivity, Re represents Reynolds number, Gr represents Grashof number and Cp represents specific heat capacity,

The non-dimensional boundary situations are as follows:

$$\Psi \neq 0; \ V=0, \Omega \neq 0; \ \theta = U=1 \text{ at } Z=1; \ 0 \leq R \leq 1;$$
$$\Psi = V = U = \theta = 0; \ \Omega \neq 0; \ at Z = 0; \ 0 \leq R \leq 1;$$
$$\theta = \Psi = V = U = 0; \ \Omega \neq 0 \text{ at } R = 0; \ 0 \leq Z \leq 1;$$
$$\Psi = \frac{\partial V}{\partial R} = \frac{\partial U}{\partial R} = \frac{\partial \theta}{\partial R} = 0; \ \Omega \neq 0 \text{ at } R=1; \ 0 \leq Z \leq 1$$

The finite difference approach is one of the best effective techniques to solve problems with nonlinear formulas (17) and (18) for vorticity and energy transport. The simultaneous system of equations was evaluated using the relaxation method. The temperature differential caused by heat transport between a fluid and a barrier is proportional to the nearby Nusselt number, as shown by equation (19).

$$Nu_z = \frac{h_z r}{k} = -\left(\frac{\partial \theta}{\partial Z}\right)_{z=1} \quad (19)$$

The typical Nusselt quantity is achieved by integrating the enclosed Nusselt amount over the distance of the heated surface, as shown in Eq. (20),:

$$N\bar{u} = \frac{\dot{Q}_{conv}}{\dot{Q}_{cond}} = -\int_0^1 \frac{\partial \theta}{\partial Z}\Big|_{Z=0\ or\ 1} dR \quad (20)$$

The stable flow requirement was achieved by setting for agreement in the vortex and temperature fields, as indicated in Eq. (21):

$$\frac{\sum_{i=1}^{N}\sum_{j=1}^{M}\left|\phi_{ij}^{n+1} - \phi_{ij}^{n}\right|}{\sum_{i=1}^{N}\sum_{j=1}^{M}\left|\phi_{ij}^{n+1}\right|} < \delta \quad (21)$$

The variable ϕ denotes Ω, Ψ or θ, and n is the number of iterations required for the outputs to converge. The value used varies between 10^{-3} and 10^{-8} in diverse kinds of literature. (Chung, 2002)

RESULTS AND DISCUSSIONS
Fig. 2 depicts the results of estimating the local Nusselt number at various convergence parameter

values varying from 10^{-1} to 10^{-8} to evaluate the impact of the convergent criterion on numerical results. It indicates that a convergence value of 10^{-4} was suitable. According to Waheed (2009), grid independence analyses demonstrated that a 41 by 41 grid design is satisfactory for outstanding simulation solutions, spatial precision, and excellent accuracy.
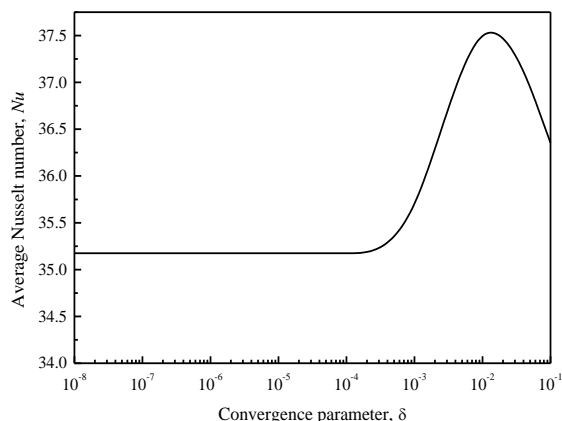

Fig. 2. A graph of the mean Nusselt number, Nu, versus convergence variable. δ

Fig. 3 illustrates the effect of altering the Richardson parameters between $2.59*10^4$ and $2.76*10^4$ on the Grasshof number. The Grasshof values are increasing in lockstep with the Richardson values, indicating that convective heat exchange is growing and the fluid is operating in the laminar region.
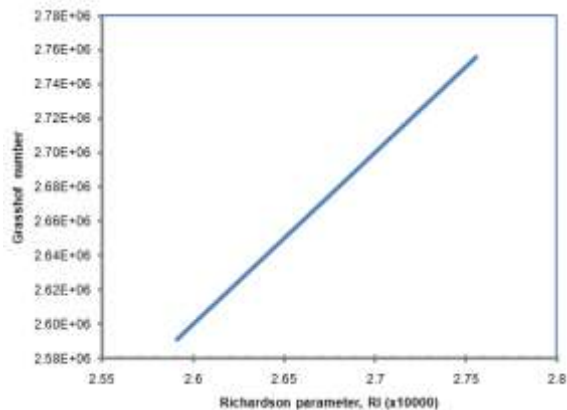

Fig. 3 The influence of altering Richardson parameter, RI on Grasshof number

Fig. 4 depicts the effect of varying Nanoparticle concentrations between 0 and 0.1 on the Richardson parameters. The maximum Richardson number is $2.76*10^4$ at a concentration of 0.04 nanoparticles. It indicates that the convective stability factor is greater than the wind speed factor while the Nanoparticle volume fraction is rapidly increasing. The outcome is that fluid turbulence in the convective heat transfer is increasing quickly whereas the convective stability

factor is decreasing. Fig. 5 shows how changing the Richardson parameters between $2.59*10^4$ and $2.76*10^4$ affect the Nusselt number. The findings revealed that Nusselt values increase in lockstep with the Richardson values. The results were consistent with those of Tiwari and Das (2007). This indicates that while conduction heat transmission is declining, convective heat transfer is rising quickly.
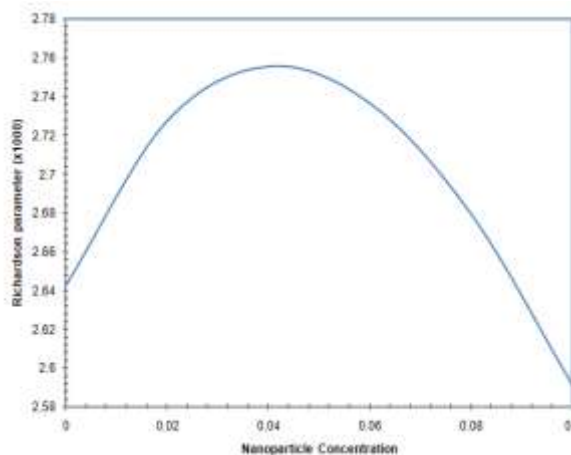

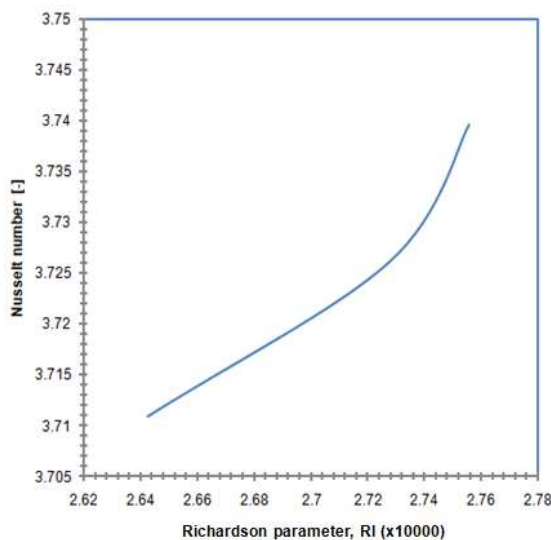Fig. 4. The effect of changeable Nanoparticle Concentration on Richardson parameter

Fig. 5 The influence of changing Richardson parameters on Nusselt number

Fig. 6 depicts the effect of varying the Richardson parameters between $2.6*10^4$ and $2.76*10^4$ on the Local Drag Coefficient. Local Drag Coefficient values decrease in lockstep with Richardson values, indicating that hydrodynamic drag is rapidly decreasing while Richardson parameters increase. A lesser drag coefficient implies that the object has a reduced amount of aerodynamic or hydrodynamic

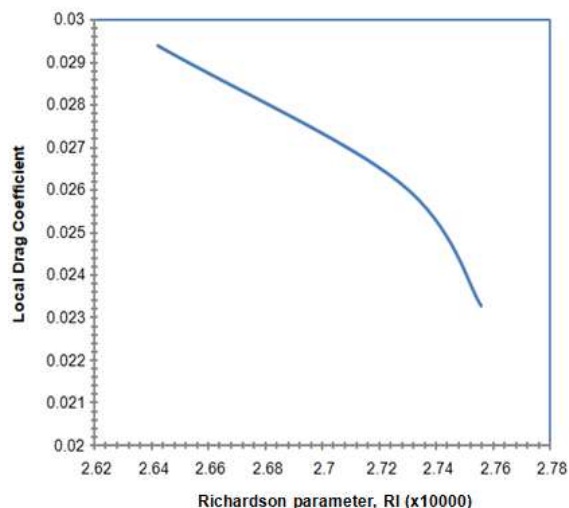drag, whereas lower Richardson values increase aerodynamic drag.

Fig. 6. The influence of changing Richardson parameters on Local Drag Coefficient

Fig. 7 illustrates the influence of Richardson parameters on the temperature of Cu nanofluid at r =0.5 along the Z-axis. The temperature distribution along z grows from 0.0 to 0.6, then remains constant until 1.0, and the temperature gradient enhances as the Richardson number of Cu nanofluid increases from $2.59*10^4$ to $2.76 *10^4$.
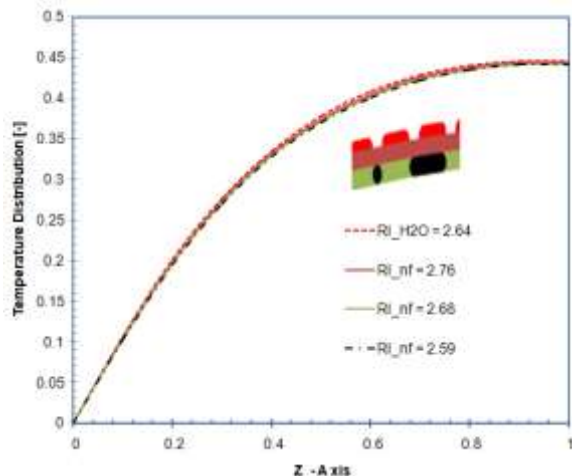

Fig. 7. Temperature curve of several Richardson parameters along the Z-axis at the plane's midpoint, r = 0.5

Fig. 8 depicts the effect of Richardson parameters ($2.59*10^4$ to $2.76 *10^4$) on the longitudinal velocity of Cu nanofluid in a plan e with r = 0.5 along the z-axis. As the Richardson value increases, the distribution of longitudinal velocity increases. It suggests that nanofluids with enhanced Richardson parameters result in enlarged laminar flow patterns. It supports the work of Al-Rashed *et al.* (2018).
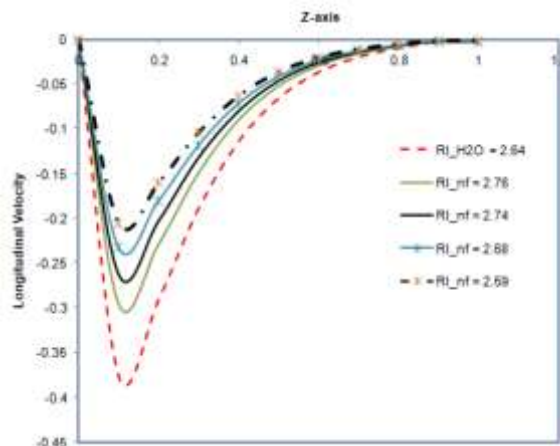

Fig. 8. Longitudinal Velocity trajectories of several Richardson parameters along the Z-axis at the centerline,

Fig. 9 shows how the Richardson parameter affects a nanofluid's vorticity. The vorticity of the nanofluid increases as the Richardson parameter increases. The vorticity distribution increases with Richardson values. This implies that flow circulation and rotation patterns are enhanced by nanofluids with increased Richardson values. Fluid rotation can be observed by circulation and vorticity, for a fluid with a finite area, a circulation is a macroscopic unit of rotation, thus a fluid rotates at any point due to a microscopic property called vorticity. The Stream function of Cu nanofluid against the number of Richardson values is displayed in Fig. 10. It shows that as Richardson values increase, the stream function of the nanofluid increases, causing an increase in the volume flow rate of the nanofluids across the tube in the laminar region.
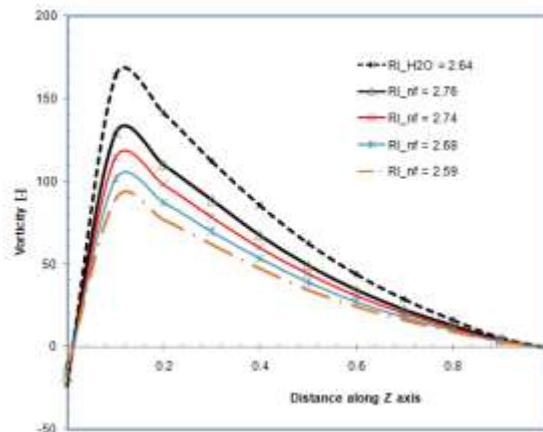

Fig. 9. Vorticity patterns for various Richardson parameters along the Z-axis at the plane's midpoint, r = 0.5
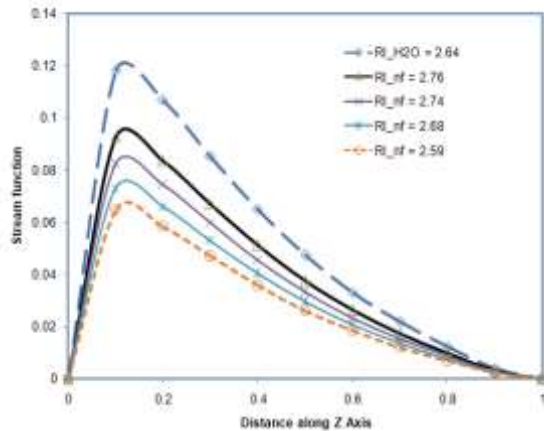
Fig. 10. Stream function curves of various Richardson parameters along the Z-axis at the centerline, r = 0.5

Conclusions: The capacity and efficiency of thermal exchangers are controlled by the heat transport fluids. The effect of Richardson factors on convective heat transfer in an enclosure with a heated Cu nanofluid-filled cylinder tube was studied using numerical simulation. The findings reveal that the Richardson attributes and nanoparticle quantities have a substantial effect on the flow and heat field. According to the findings, the temperature gradient of nanofluids grows as Richardson parameters rise. The stream function, longitudinal velocity, rotation, and circulation all increase as Richardson values increase. This study illustrates that Richardson-driven nanoparticle inclusion affects the temperature and flow pattern of a solution, hence modifying its utility.

REFERENCES

Al-Rashed, AAAA; Kalidasan, K; Kolsi, L; Velkennedy, R; Aydi, A; Hussein, AK; Malekshah, EH (2018). Mixed convection and entropy generation in a nanofluid-filled cubical open cavity with a central isothermal block. *Int. J. Mech. Sci*. 135, 362–375.

Basak, T; Roy, S; Sharma, PK; Pop, I (2009)**.** Analysis of mixed convection flows within a square cavity with uniform and non-uniform heating of the bottom wall. *Int. J. Therm. Sci*. 48, 891–912.

Billah, MM; Rahman, MM; Razzak, MA; Saidur, R; Mekhilef, S (2013) Unsteady buoyancy-driven heat transfer enhancement of nanofluids in an inclined triangular enclosure. *Int. Commun. Heat Mass Transf*. 49, 115–127.

Choi, SUS; Eastman, JA (1995). Enhancing thermal conductivity of fluids with nanoparticles. In Proceedings of the International Mechanical Engineering Congress and Exhibition, San Francisco, CA, USA, 12–17

Chung, TJ (2002) Computational Fluid Dynamics. Cambridge University Press, Cambridge.

Hussain, S; Ahmad, S; Mehmood, K; Sagheer, M (2017)**.** Effects of inclination angle on mixed convective nanofluid flow in a double lid-driven cavity with discrete heat sources. *Int. J. Heat Mass Transf*. 106, 847–860.

Kalbasi, M; Saeedi, A (2012) "Numerical Investigation into the Convective Heat Transfer of CuO Nanofluids Flowing Through a Straight Tube with Uniform Heat Flux," *Indian Journal of Science and Technology* 5, pp. 2455-2458, Iran;

Kareem, AK; Gao, S (2017). Mixed convection heat transfer of turbulent flow in a three-dimensional lid-driven cavity with a rotating cylinder. *Int. J. Heat Mass Transf.* 112, 185–200.

Khanafer, K; Aithal, SM (2017). Mixed convection heat transfer in a lid-driven cavity with a rotating circular cylinder. *Int. Commun. Heat Mass Transf.* 86, 131–142.

Khodadadi, JM; Hosseinizadeh, SF (2007). Nanoparticle-enhanced phase change materials (NEPCM) with great potential for improved thermal energy storage. *Int. Commun. Heat Mass Transf.* 34, 534–543.

Lin, YH; Kang, SW; Chen, HL; (2008).Effect of silver nano-fluid on pulsating heat pipe thermal performance. *Appl. Therm. Eng*., 28, 1312–1317.

Mastiani, M; Kim, MM; Nematollahi, A (2017). Density maximum effects on mixed convection in a square lid-driven enclosure filled with Cu-water nanofluids. *Adv. Powder Technol*. 28, 197–214.

Mastiani, M; Sebti, SS; Mirzaei, H; Kashani, S; Sohrabi, A (2015). Numerical study of melting in an annular enclosure filled with nano-enhanced phase change material. *Therm. Sci.,* 19, 1067–1076.

Meymian, NZ; Clark, NN; Musho, T; Darzi, M; Johnson, D; Famouri, P (2018). An optimization method for flexural bearing design for high-stroke high-frequency applications. *Cryogenics* 95, 82–94.

Nasrin, R; Parvin, S (2012). Investigation of buoyancy-driven flow and heat transfer in a trapezoidal cavity filled with water-Cu nanofluid. Int. Commun. Heat Mass Transf. 39, 270–274.

Nguyen-Thoi, T; Bhatti, MM; Ali, JA; Hamad, SM; Sheikholeslami, M; Shafee, A; Haq, R (2019) Analysis on the heat storage unit through a Y-shaped fin for solidification of NEPCM. *J. Mol. Liq.* 292, 111378.

Patankar, SV (1980). Numerical heat transfer and fluid flow (Hemisphere Series on Computational Methods in Mechanics and Thermal Science; Hemisphere Publishing Corporation (CRC Press, Taylor & Francis Group): Boca Raton, FL, USA.

Sangotayo E. O.and Hunge O. N. (2019). Numerical Analysis of Nanoparticle concentration Effect on Thermo-physical Properties of Nanofluid in a Square Cavity, *proceeding of WRFASE International Conference*, Abu Dhabi-UAE, pp. 5-10

Selimefendigil, F; Öztop, HF (2018). Mixed convection of nanofluids in a three-dimensional cavity with two adiabatic inner rotating cylinders. *Int. J. Heat Mass Transf.* 117, 331–343.

Sheikholeslami, M; Rokni, HB (2017). Nanofluid two-phase model analysis in the existence of induced magnetic field. *Int. J. Heat Mass Transf.* 107, 288–299.

Sheremet, MA; Pop, I (2015). Mixed convection in a lid-driven square cavity filled by a nanofluid: Buongiorno's mathematical model. *Appl. Math. Comput.* 266, 792–808.

Tiwari, RK; Das, MK (2007). Heat transfer augmentation in a two-sided lid-driven differentially heated square cavity utilizing nanofluids. *Int. J. Heat Mass Transf*. 50, 2002–2018.

Umavathi, JC; Bég, OA, (2021) Augmentation of heat transfer via nanofluids in duct flows using Fourier-type conditions: Theoretical and numerical study, Proceedings of the Institution of Mechanical Engineers, Part E: *Journal of Process Mechanical Engineering,* pp 1-40

Waheed, MA (2009) "Mixed convective heat transfer in rectangular enclosures driven by a continuously moving horizontal plate". *International Journal of Heat and Mass Transfer*, 52, pp. 5055–5063.

Waqas, H; Khan, SU; Imran, M; Bhatti, MM (2019). Thermally developed Falkner–Skanbioconvection flow of a magnetized nanofluid in the presence of a motile gyrotactic microorganism: Buongiorno'snanofluid model. *Phys. Scr*. 94, 115304.

Yousif, MA; Ismael, HF; Abbas, T; Ellahi, R (2019)**.** Numerical study of momentum and heat transfer of MHD carreau-nanofluid over an exponentially stretched plate with internal heat source/sink and radiation. *Heat Transf. Res.* 50, 649–658.

Taylor, RA; Phelan, PE; Otanicar, TP; Walker, CA; Nguyen, M; Trimble, S; Prasher, R (2011)**.** Applicability of nanofluids in high flux solar collectors. J. Renew. Sustain. Energy, 3, 023104.